3'-Deoxy-3'-[18F]Fluorothymidine Positron Emission Tomography Imaging of Thymidine Kinase 1 Activity After 5-Fluorouracil Treatment in a Mouse Tumor Model

IL KI HONG[1], SEOG YOUNG KIM[2], JIN HWA CHUNG[2], SEUNG JIN LEE[3], SEUNG JUN OH[2,4], SANG JU LEE[2,4], JUNGSU OH[2,4], JIN-SOOK RYU[2,4], TAE WON KIM[5], DEOG YOON KIM[1] and DAE HYUK MOON[2,4]

[1]Department of Nuclear Medicine, Kyung Hee University Medical Center, School of Medicine, Kyung Hee University, Seoul, Republic of Korea;
[2]Molecular Imaging Research, Biomedical Research Center, Asan Institute for Life Sciences, Asan Medical Center, Seoul, Republic of Korea;
[3]College of Pharmacy, Gachon University, Incheon, Republic of Korea;
Department of [4]Nuclear Medicine and [5]Oncology, Asan Medical Center, University of Ulsan College of Medicine, Seoul, Republic of Korea

Abstract. *Aim: We aimed to investigate whether 3'-deoxy-3'-[18F]fluorothymidine ([18F]FLT) positron emission tomography (PET) can estimate thymidine kinase 1 (TK1) activity after thymidylate synthase (TS) inhibition by 5-fluorouracil (5-FU) in a mouse tumor model. Materials and Methods: Nude mice with HT29 tumors were injected with phosphate-buffered saline or 5-FU (16.7 or 50 mg/kg). Twenty-four hours later, 2-hour dynamic images were acquired after injection of [18F]FLT. In another group of mice with HT29 cells, static PET images were obtained 110 min after [18F]FLT injection. Results: Kinetic parameters related to [18F]FLT retention increased significantly, whereas the de-phosphorylation of [18F]FLT monophosphate decreased significantly. The standardized uptake value (SUV_{mean}) of HT29 tumors correlated significantly with the net influx constant and the distribution volume for phosphorylated [18F]FLT. There was a significant correlation between the tumor SUV_{mean} and TK1 activity. Conclusion: SUV_{mean} at 110-120 min after [18F]FLT, can quantitatively evaluate kinetic parameters and TK1 activity after TS inhibition.*

Correspondence to: Dae Hyuk Moon, MD, Department of Nuclear Medicine, Asan Medical Center, University of Ulsan College of Medicine, 88 Olympic-ro 43-gil, Songpa-gu, Seoul 138-736, Republic of Korea. Tel: +82 230104592, Fax: +82 230104588, e-mail: dhmoon@amc.seoul.kr

Key Words: 3'-deoxy-3'-[18F]fluorothymidine, positron emission tomography, thymidine kinase, 5-fluorouracil, thymidylate synthase.

Thymidylate synthase (TS), a critical enzyme in the *de novo* synthesis of 2'-deoxythymidine-5'-monophosphate, is a target for TS inhibitors. Pyrimidines (*e.g.*, 5-fluorouracil [5-FU] and 5-fluorodeoxyuridine) and folate cosubstrates (*e.g.*, raltitrexed, pemetrexed, and nolatrexed) inhibit TS as a cancer chemotherapeutic target (1, 2). However, the overall response rate of 5-FU when used as a single chemotherapeutic agent is only 10-15% in advanced colorectal cancer, and 20-40% when used as part of combination regimens with leucovorin, dihydropyrimidine dehydrogenase, methotrexate, and interferon (3, 4). Identifying a sub-group of patients who might benefit from TS inhibitors is, therefore, important.

Quantification of TS inhibition in tumors currently relies on measurements of biochemical changes that accompany TS inhibition. TS inhibition leads to an increase in intracellular pools of the TS substrate dUMP and its corresponding nucleoside 2'-deoxyuridine. Plasma levels of 2'-deoxyuridine, intra-tumoral TS activity, and measurement of dUMP binding sites have been used as pharmacodynamic markers of TS inhibitor activity (5, 6). However, plasma assays do not provide a direct assessment of TS inhibition within a tumor, and tumor biopsy may not always be possible due to significant morbidity.

Substrate cycles, involving phosphorylation of deoxyribonucleosides by kinases and de-phosphorylation of deoxyribonucleoside 5'-phosphates by a nucleotidase, participate in regulation of the size of pyrimidine deoxyribonucleoside triphosphate pools (7). TS inhibitors can cause a rapid decrease in thymidine phosphate pools. Cancer cells respond to decrease in thymidine phosphate pools by an increase in thymidine kinase

1 (TK1), and nucleoside transporter (8) or possibly by decrease in 5'(3')-deoxyribonucleotidase activity (7, 9) to increase phosphorylation of nucleosides. Positron emission tomography (PET) studies with 3'-deoxy-3'-[^{18}F]fluorothymidine ([^{18}F]FLT) have demonstrated an increase in [^{18}F]FLT uptake after TS inhibition (10-12). Underlying biochemical features associated with the increase in [^{18}F]FLT uptake in tumors were shown to be re-distribution of nucleoside transporters (13) and an increase in TK1 levels (14). The temporary increase in [^{18}F]FLT retention, referred to as the flare effect, may be used in pharmacodynamic measurements of the effect of TS inhibitors (11, 15).

Recently, we showed that [^{18}F]FLT flare was associated with poor treatment response in patients with metastatic colorectal cancer (16). [^{18}F]FLT flare may indicate that a salvage pathway would circumvent the inhibition of pathways of *de novo* synthesis (17). Evidence of the contribution of the salvage pathway to clinical resistance to TS inhibition may include reduced activity of TS inhibitors in the presence of extracellular thymidine (18), enhancement of the anticancer activity of 5-FU after thymidine transport inhibition (19), and increased activity of TS inhibition in thymidine kinase–deficient tumors (20).

Thymidine metabolism following TS inhibition, and its effect on [^{18}F]FLT metabolism must be elucidated before [^{18}F]FLT metabolism can be adopted as an imaging biomarker for TS inhibition. TK1 is the key regulator of [^{18}F]FLT retention. Nevertheless, the relationship between TK1 activity and [^{18}F]FLT uptake after TS inhibition is not entirely clear. Furthermore, TS inhibition may result in changes in perfusion, and biodistribution of [^{18}F]FLT in addition to nucleoside transporter and enzymes for thymidine metabolism (21). Therefore, we aimed to study the kinetic modeling of [^{18}F]FLT using compartmental analysis to fully-characterize the kinetics of [^{18}F]FLT in tumor tissue after 5-FU treatment in a mouse tumor model. We also assessed whether a simple semi-quantitative method, the standardized uptake value (SUV), can estimate kinetic parameters from validated compartmental models and TK1 after TS inhibition by 5-FU.

Materials and Methods

Radiopharmaceutical preparation. [^{18}F]FLT was prepared from 5'-O-(DMTr-2'-deoxy-3'-O-nosyl-β-D-threopentafuranosyl)-3-N-BOC-thymine by nucleophilic [^{18}F]fluorination in *t*-amyl alcohol (22). Radiochemical yields (non decay corrected) and purity were 44.9% ± 3.2% and 99.8% ± 1.1%, respectively. The specific activity of the obtained [^{18}F]FLT was 197 ± 53 TBq/mmol.

Cell cultures and tumor models. HT29 cell line was obtained from the American Type Culture Collection (Rockville, MD, USA). Cells were routinely cultured in RPMI-1640, supplemented with 10% heat-inactivated fetal bovine serum, L-glutamine (2 mM), penicillin (50 IU/mL), and streptomycin (50 μg/mL). Cells were maintained at 37˚C in an atmosphere of 5% CO_2 in air. Cell lysates were prepared as described previously (14). Protein content was determined by the Bradford assay (Bio-Rad, Hercules, CA, USA).

Athymic male Balb-c/nu mice (age, 6 weeks; weight, 20-30 g) were purchased from Japan Shizuoka Laboratory Center (Hamamatsu, Japan). The research protocol was approved by the Institutional Animal Care and Use Committee at the Asan Institute for Life Science. Mice were maintained in accordance with the guideline issued by this committee. Exponentially growing cells (0.2 ml containing 1×10^7 cells) were inoculated into the right flank of each mouse. Tumor volumes were measured with calipers and calculated according to the following formula: volume=$(\pi/6)abc$, where a, b, and c represent the three orthogonal axes of the tumor, respectively. When tumor volumes reached 80-120 mm^3 after injection, mice were subjected to animal PET imaging and TK1 activity analysis.

Animal PET imaging with [^{18}F]FLT after vehicle or 5-FU injection. Mice with HT29 tumors were injected intraperitoneally with a bolus of phosphate-buffered saline (n=7), or 5-FU (Choongwae Pharma Corporation, Seoul, Korea; 16.7 or 50 mg/kg; n=6 for each group). 5-FU doses were chosen based on the results of previous studies on the anti-tumor and adverse effects of 5-FU in mice with human xenograft (23, 24). Twenty-four h later, 2-h dynamic PET images were acquired after tail vein injection of 7.4 MBq (0.2 mCi) of [^{18}F]FLT using a commercially available PET system (microPET Focus 120 system, Siemens Medical Solutions, Inc., Knoxville, TN, USA) (25). A 37-frame dynamic protocol (4×3 s, 6×1 s, 7×6 s, 8×30 s, 1×300 s, and 11×600 s) was used for the emission scans with 128×128×95 matrices and voxel size of 0.432×0.432×0.796 mm. The intraperitoneal injection was expected to result in slow absorption of 5-FU from the peritoneal cavity, allowing mice to be exposed to 5-FU for prolonged periods of time (26). Mice were maintained under isoflurane anesthesia during the uptake and scanning periods. A heating pad and heat lamp were used to maintain body temperature at about 37˚C using a rectal probe. PET images were reconstructed by filtered back projection using a Hamming filter at a cut-off frequency of 0.5 cycles per pixel. No attenuation correction was applied.

Another group of 19 mice with HT29 tumors were injected with phosphate-buffered saline (n=7), or 5-FU (16.7 mg/kg, n=6; and 50 mg/kg, n=6). Twenty-four h later, a static PET imaging was performed 110 min after injection of 7.4 MBq (0.2 mCi) of [^{18}F]FLT for 10 min. In this group of mice, TK1 activity in tumors was measured after PET imaging.

Analysis of [^{18}F]FLT PET. To obtain time-activity curves for kinetic analysis, cylindrical volumes-of-interest (VOIs) with a diameter of seven pixels and a length of three slices were drawn in the left ventricle (LV) on the early frame. LV time-activity curves corrected for partial-volume effects with the correction factor described were used as the input function (27). The last frame of the dynamic acquisition was used to define the VOI for analysis of [^{18}F]FLT activity in tumors as described previously (28).

To determine the optimal compartment model for [^{18}F]FLT PET in mice with HT29 tumors, we tested a 3-compartment model and its simplified models (29). The three-compartment model includes the parameters K_1, K_1/k_2, k_3, k_4. Parameters K_1 and k_2 are rate constants for influx and efflux of [^{18}F]FLT between plasma and the tissue pool, respectively. The rate constant k_3 represents TK1-

mediated phosphorylation of [^{18}F]FLT. The parameter k_4 represents dephosphorylation of [^{18}F]FLT-phosphate. The blood volume fraction (V_b) was included in the modeling. Three-compartment models with reversible phosphorylation ($k_4 \neq 0$, 3C5P) and irreversible phosphorylation ($k_4=0$, 3C4P) were examined. In addition, a 2-compartment model that combined exchangeable and phosphorylated compartments into a single tissue compartment with three parameters (2C3P: K_1, k_2, and V_b) was also considered.

Data analysis was performed using PMOD software package (version 2.65; PMOD Technologies, Zurich, Switzerland). Tissue time-activity curves were fitted to the models using the nonlinear least-squares method with the Levenberg-marquardt algorithm, which minimizes the weighted sum of squared error between PET measurements and model solutions. Estimated parameters were restricted to the following value ranges: 0.05-1.0 for K_1, 0.1-10.0 for K_1/k_2, 0.001-1.0 for k_3, 0.001-0.2 for k_4, and 0.01-0.2 for V_b. Initial values for K_1, K_1/k_2, k_3, k_4, and V_b were set at 0.1, 1.0, 0.1, 0.01, and 0.05, respectively. The net influx constant (K_{FLT}), and the distribution volume for phosphorylated [^{18}F]FLT nucleotides (DVm) were estimated as follows:

$K_{FLT}=K_1 k_3 / (k_2 + k_3) = K_1 k_3 / (K_1/V_d + k_3)$ where V_d is the early volume of distribution of the reversible compartment, which is given by K_1/k_2 according to previous reports (29, 30), and

$DV_m=K_1/k_2 \times (k_3/k_4)$.

We chose an adequate compartment model on the basis of the Akaike's information criterion (AIC) and extra sum-of-squares F test.

For semi-quantitive analysis, the same VOIs for kinetic analysis were used. The mean standardized uptake value (SUV_{mean}) of each tumor was calculated using the following formula: SUV_{mean}=(tumor radioactivity in the tumor VOI, measured as Bq/cc × body weight) divided by injected radioactivity. We examined the correlations between kinetic parameters and SUV_{mean}.

TK1 activity assay. TK1 activity was measured as previously described (14). Tumors were lysed in lysis buffer and incubated for 30 min on ice. Lysates were centrifuged at 10,000 g for 20 min at 4˚C, and supernatants were centrifuged again at 100,000 ×g for 1 h at 4˚C, to separate mitochondrial fractions. After protein contents were determined, cytosolic fractions were assayed for TK1 activities in a reaction buffer containing 10 μM [Methyl-^{3}H]-thymidine (740 GBq/mmol, Perkin Elmer, MA, USA). Mixtures were then incubated at 37˚C with gentle stirring, and samples were removed and added to 5 mM ethylenediaminetetraacetic acid to stop the reaction at 15, 30, and 60 min. For sequestration of labeled nucleotides, each sample was spotted onto DE-81 filters (Whatman, GE healthcare, NJ, USA), dried, and washed in 4 mM ammonium formate and 95% ethanol. Radioactivity was measured by liquid scintillation counting with Ultima Gold F scintillation cocktail solution (Perkinelmer, MA, USA). Activities were calculated with linear time-activity curves and are presented as picomoles of phosphorylated thymidine/minute/mg protein.

Statistical analysis. Data are expressed as mean (SD). The Kruskal-Wallis test was used to assess significant differences among groups, and different treatment groups were compared using the Mann-Whitney test with *post-hoc* Bonferroni correction. Repeated measurements of analysis of variance with three levels (vehicle and two doses of 5-FU) were used to test the changes in SUV_{mean} between the groups at three different time points (50, 80, and 110 min) after vehicle or 5-FU injection. Correlations were assessed by using Spearman's rank correlation coefficient. $p<0.05$ was considered to indicate statistical significance. All statistical analyses were conducted by using the IBM SPSS Statistics Version 19 for Windows (SPSS Inc., IBM Company, Somers, NY, USA) statistical package.

Results

Compartment modeling. Figure 1 shows axial and coronal PET images obtained 110 min after [^{18}F]FLT injection, and time-activity curves for HT29 tumors and left ventricular blood pool. Mice injected with vehicle had a low level of [^{18}F]FLT retention (Figure 1A). On the other hand, 5-FU injected mice showed a high level of [^{18}F]FLT retention (Figures 1B and C). Mice injected with 50 mg/kg 5-FU had a continuous accumulation of [^{18}F]FLT in the HT29 tumors over the entire 2 h measurement period (Figure 1C).

Time-activity curves were fitted more accurately when V_b was included in the model (3-compartment model with reversible phosphorylation; $k_4 \neq 0$, 3C5P) in both vehicle and 5-FU treatment group. AIC values from the 3C5P models were lower than those from the 3C4P and 2C3P models in all mice except for two (Table I). The results of F tests were similar to those of AIC analysis.

Correlation matrices for the 3C5P model are shown in Table II. In both vehicle and 5-FU treatment groups, K_1/k_2 and k_3 were highly correlated, and in vehicle treated mice there was also a high correlation between k_3 and k_4.

Parameters for [^{18}F]FLT uptake in HT29 tumors after vehicle or 5-FU treatment. Figure 2 shows the mean and SD of kinetic parameters estimated with the 3C5P models, and SUV_{mean} of HT29 tumors. Kinetic parameters related to [^{18}F]FLT retention (K_1/k_2 and k_3) were significantly different between the groups ($p<0.005$; Figures 2B and C). K_1/k_2 and k_3 parameters in 5-FU treated mice were higher, but there was no difference in V_b and K_1 (Figure 2A). The k_4 parameter, defining the dephosphorylation of [^{18}F]FLT monophosphate, was also significantly different ($p<0.01$) between the groups with a lower value in the 5-FU treatment groups (Figure 2D). As a result, the kinetic macroparameters (K_{FLT} and DV_m) increased dose-dependently with 5-FU treatment (Figures 2E and 2F). The SUV_{mean} of HT29 tumors at 50 and 110 min after [^{18}F]FLT administration also showed a dose-dependent increase following 5-FU treatment (Figures 2G and 2H).

The changes in SUV_{mean} at three different time points (50, 80, and 110 min) after injection of vehicle or 5-FU were significantly different between vehicle or 5-FU treated mice (Figures 2G and 2H, $p<0.001$). Mice injected with 50 mg/kg 5-FU showed significantly increasing SUV_{mean} up to 110 min after the injection, whereas mice injected with vehicle had significantly decreasing SUV_{mean} over time ($p<0.001$). The SUV_{mean} of HT29 tumors at 110 min after [^{18}F]FLT administration correlated significantly with K_{FLT} ($\varrho=0.959$, $p<0.001$) and DV_m ($\varrho=0.905$, $p<0.001$).

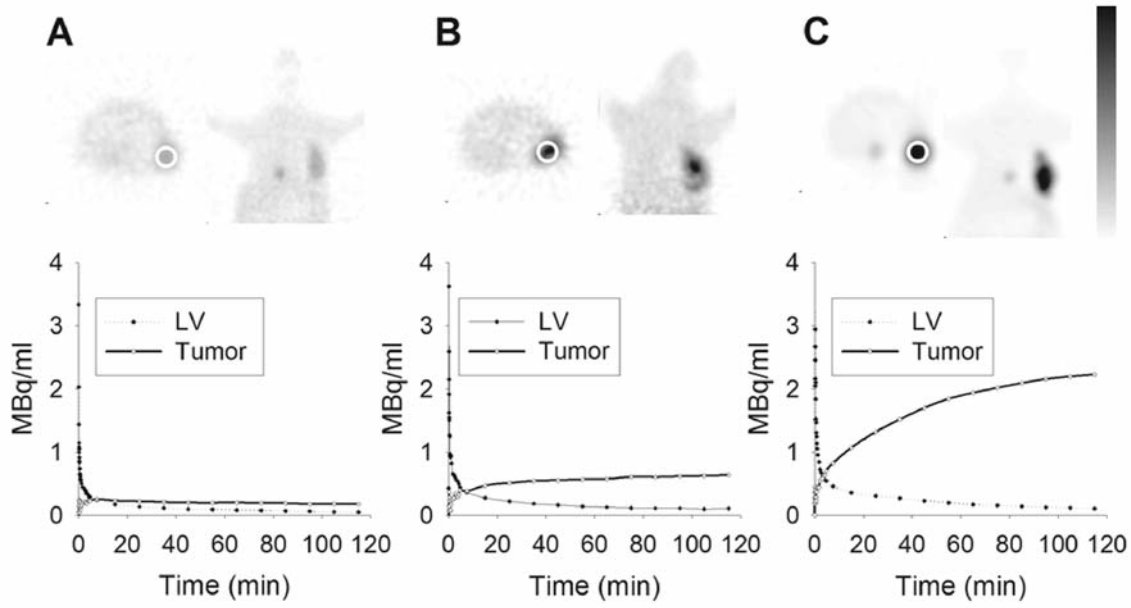

Figure 1. *Typical [^{18}F]FLT PET images of mice with HT29 tumors and time-activity curves. PET images obtained at 110-120 min after injection of 7.4 MBq of [^{18}F]FLT and time-activity curves for left ventricular (LV) and HT29 tumor-bearing regions in vehicle (A), 16.7 (B), and 50.0 mg/kg (C) 5-FU treated mice under isoflurane anesthesia. High [^{18}F]FLT activity in the tumor was seen following 5-FU treatment. Mice treated with 50.0 mg/kg of 5-FU showed a continuous accumulation of [^{18}F]FLT in the tumors. LV input function and tissue time–activity curves were obtained from VOIs drawn on the left ventricle and tumor-bearing regions (white circle) for kinetic analysis.*

Correlation of [^{18}F]FLT uptake and TK1 activity. The tumor SUV_{mean} of vehicle, 16.7 mg/kg and 50 mg/kg 5-FU-treated mice-determined by static imaging of [^{18}F]FLT PET, as was significantly different between groups ($p<0.005$, Figure 3). Similarly, TK1 activity was also significantly different between the treatment groups ($p<0.001$, Figure 3). A significant correlation was observed between the tumor [^{18}F]FLT uptake (SUV_{mean}) obtained with the static PET images and TK1 activity ($\varrho=0.890$, $p<0.001$, Figure 3).

Discussion

In the present study, we examined the kinetics of [^{18}F]FLT uptake in HT29 tumors after 5-FU treatment. Our results showed that the tissue time-activity curves of tumor-bearing regions in vehicle and 5-FU-treated groups were best-described by the 3C5P model. The rate constants related to [^{18}F]FLT retention increased with 5-FU treatment. The k_4 parameter, representing de-phosphorylation of phosphorylated [^{18}F]FLT, decreased significantly in the 5-FU treated group. The SUV_{mean} showed a high correlation with kinetic parameters from validated compartmental models (K_{FLT} and DV_m) as well as TK1 after TS inhibition by 5-FU. Our results suggest that TS inhibition after 5-FU treatment can be assessed quantitatively with [^{18}F]FLT PET.

The most important finding in the present study is that the kinetic parameters related to [^{18}F]FLT retention, including K_1/k_2, k_3, and macroparameters, increased after 5-FU. Although the high levels of co-variance between K_1/k_2 and k_3 parameters make it difficult to obtain independent estimates, our results may be in agreement with previous studies demonstrating an increased TK1 activity after TS inhibition (8, 14). Our *ex vivo* study of HT29 tumors consistently confirmed an increase in TK1 activity. However, K_1, which is representative of nucleoside transport, did not change after 5-FU treatment. We administered 5-FU by intraperitoneal injection to allow mice exposure to 5-FU for a prolonged period of time (26). In our previous work, we found that [^{18}F]FLT PET may be optimal after 24 h of treatment when continuous infusion of 5-FU is given, because of a higher [^{18}F]FLT flare than that after 1-2 h (14). The [^{18}F]FLT flare observed early after TS inhibition may be largely due to the re-distribution of the nucleoside transporter (10, 13). On the other hand, our study suggests that the effect of increased TK1 activity may predominate later. The absence of change in K_1 in our study may be explained by [^{18}F]FLT imaging being carried out 24 h after 5-FU injection.

The present study showed that k_4, which represents a significant loss of phosphorylated [^{18}F]FLT nucleotides by de-phosphorylation, was lower than k_3, but it should not be

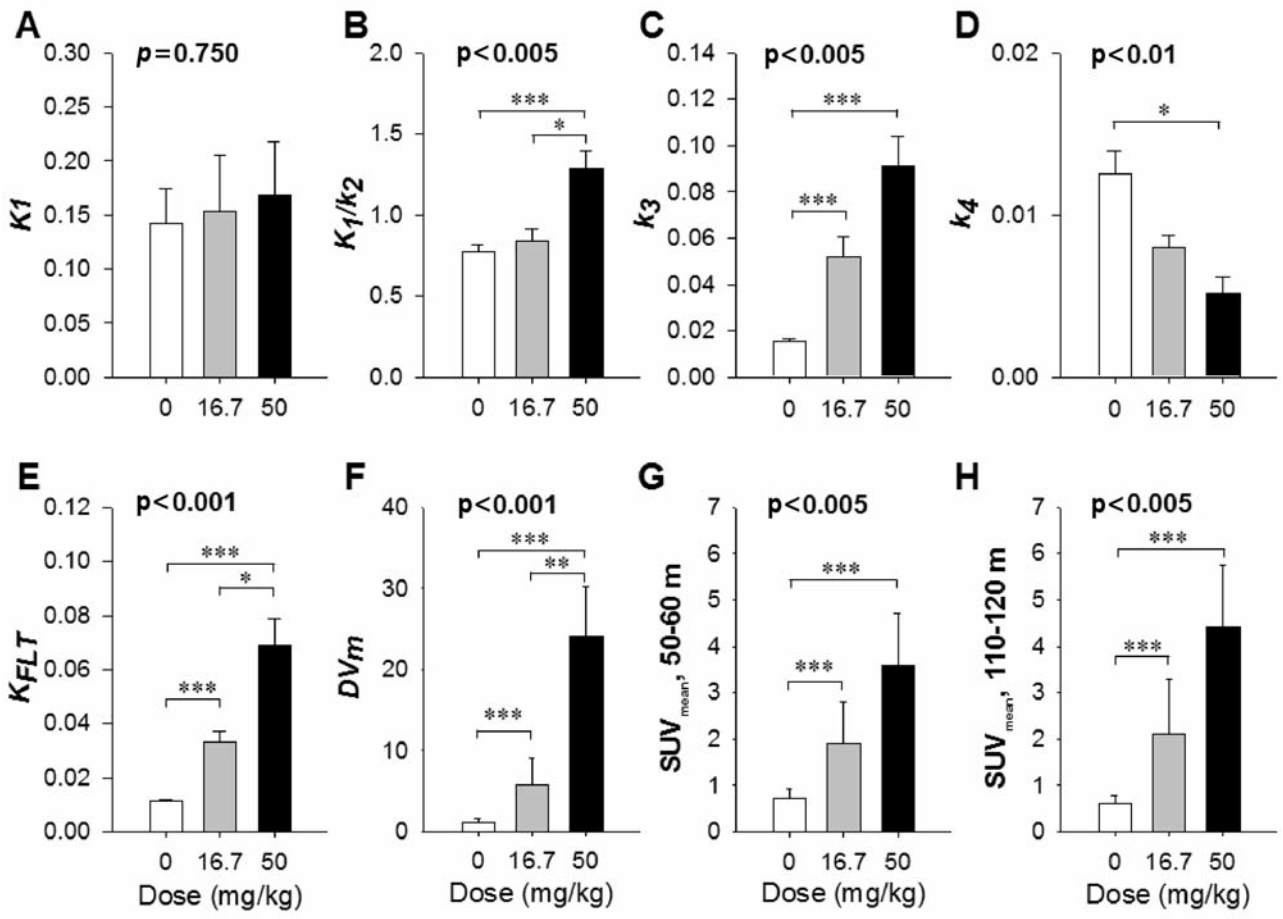

Figure 2. *Kinetic and static parameters of [^{18}F]FLT PET in mice with HT29 tumors obtained by 2 h dynamic imaging 24 h after saline, 16.7 and 50 mg/kg 5-FU treatment. Data are expressed as mean±SD. All parameters except K_1 were significantly different between the three groups. Only p-values that were significant with post-hoc Bonferroni correction are shown: *p<0.05, **p<0.01, ***p<0.005). Dose-dependent increase in K_{FLT}, DV_m and SUV_{mean} was observed with 5-FU treatment.*

ignored in the kinetic modeling of HT29 tumors. Importantly, there was a significant decrease in k_4 after 5-FU treatment. The decrease in k_4 after 5-FU treatment may not be related to a correlation with k_3 because no high level of covariance was observed in the 5-FU treatment group. Dephosphorylation of phosphorylated [^{18}F]FLT nucleotides is catalyzed by 5'(3')-deoxyribonucleotidase. A decrease in 5'(3')-deoxyribonucleotidase activity leads to increased phosphorylation of nucleosides. The 5'(3')-deoxyribonucleotidase is a regulator of nucleoside and drug metabolism, and a change in 5'(3')-deoxyribonucleotidase activity is associated with nucleoside analogue activation and drug resistance (31). Our findings suggest a role for 5'(3')-deoxyribonucleotidase activity in the effect of 5-FU-mediated suppression of the *de novo* pathway on the salvage pathway. Among the macrokinetic parameters that can be reproducibly measured from kinetic modeling of [^{18}F]FLT (28), K_{FLT} is calculated on the basis of the assumption that k_4 can be ignored. Therefore, DV_m may be a better macrokinetic parameter with which to assess [^{18}F]FLT kinetics after TS inhibition.

The present study demonstrates that [^{18}F]FLT PET parameters with 3C5P model are most suitable for evaluating the effect of 5-FU in HT29 tumors. The most simple method used to quantify [^{18}F]FLT uptake is SUV measurement, which is relevant for routine clinical use. SUV analysis, however, can yield misleading results through the contribution of non-phosphorylated [^{18}F]FLT and washout of phosphorylated [^{18}F]FLT by k_4 when imaged at later time points (32). Our dynamic [^{18}F]FLT PET revealed a significant decrease in k_4, which was accompanied by significantly increasing SUV_{mean} up to 110 min after 5-FU. Therefore, SUV at later time points could be a simple measure of [^{18}F]FLT metabolism after 5-FU treatment. We

Table I. *Comparison of kinetic models for [18F]FLT PET in mice implanted with HT29 tumors using the Akaike's information criterion (AIC) and extra sum-of-squares F-test.*

5-FU (mg/kg)	Mouse number	AIC			*F* ratio (A *vs.* B)	
		3C5P (A)	3C4P (B)	exp((A –B)/2)		*p*-Value
Vehicle	1	347.9	345.6	1	1.7	0.069
	2	254.1	289.0	<0.001	13.9	<0.001
	3	259.5	283.3	<0.001	1.6	0.100
	4	252.0	280.1	<0.001	10.0	<0.001
	5	254.3	276.9	<0.001	2.6	0.004
	6	244.6	263.1	<0.001	7.0	<0.001
	7	240.2	268.0	<0.001	2.6	0.004
16.7	1	252.3	287.9	<0.001	10.6	<0.001
	2	235.8	287.6	<0.001	19.6	<0.001
	3	263.2	285.2	<0.001	6.4	<0.001
	4	271.5	281.2	0.008	2.0	0.022
	5	209.3	249.2	<0.001	69.2	<0.001
	6	196.8	224.6	<0.001	25.4	<0.001
50	1	271.1	289.1	<0.001	17.4	<0.001
	2	231.9	278.3	<0.001	14.7	<0.001
	3	252.7	280.1	<0.001	22.7	<0.001
	4	287.9	284.5	1	2.5	0.005
	5	257.6	270.6	0.002	8.1	<0.001
	6	250.2	267.9	<0.001	3.9	<0.001

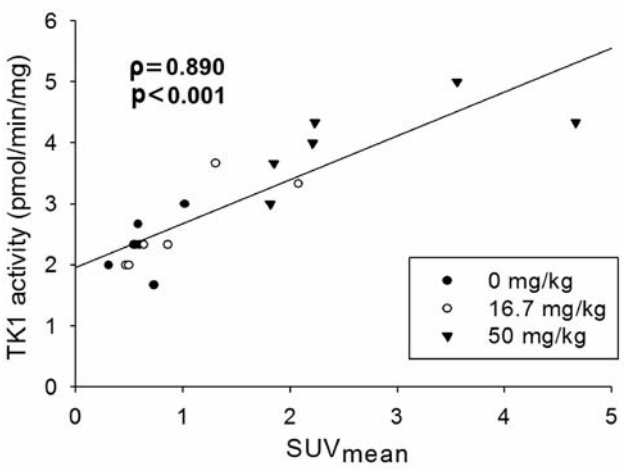

Figure 3. *Estimated correlation of tumoral [18F]FLT uptake 110 min after [18F]FLT injection and TK1 activity in mice with HT29 tumors (ρ=0.890, p<0.001). [18F]FLT uptake measurements were obtained 24 h after intraperitoneal injection of vehicle or 5-FU.*

validated SUV_{mean} at 110-120 min after 5-FU treatment as a measure of the pharmacodynamic effect, by demonstrating a high correlation with K_{FLT} and DV_m. Finally, we demonstrated a high correlation of SUV_{mean} at 110-120 min with TK1 activity in HT29 tumors.

A limitation of this study is that we did not evaluate [18F]FLT kinetics after a high effective dose of 165 mg/kg 5-FU (13, 21). In contrast to our results, previous studies have found a decreased [3H]thymidine or [18F]FLT uptake in RIF-1 and HT29 tumors associated with decreased cell viability after a high dose of 5-FU (21, 33). Since compromised cell viability may obscure [18F]FLT flare by 24 h after 5-FU injection, we used lower doses of 5-FU. A more comprehensive study that includes the effect of cell viability on [18F]FLT uptake in addition to TS inhibition is needed. Secondly, our results are applicable only to infusional 5-FU treatment. The timing of [18F]FLT PET after TS inhibition and analysis approaches should be optimized and validated to quantitatively evaluate TS inhibition by other TS inhibitors. Thirdly, our mouse model may not be valid in this situation because of high blood thymidine level enough to cause significant competitive inhibition of [18F]FLT uptake. However, induction of TK1 and cell-cycle transition after 5-FU has been demonstrated as a mechanism for [18F]FLT PET in mice models including HT29 in our previous study (14). In mice, left ventricular activity can be used as an image-derived input function because no [18F]FLT metabolites are found in the plasma (27). Mice models may be more suitable for dynamic imaging analysis. Finally, it was beyond the scope of our study to evaluate quantitative [18F]FLT PET parameters as predictive markers of response to 5-FU.

Conclusion

The three-compartment model with reversible phosphorylation best described the tissue time-activity curves of the tumor-bearing regions in vehicle and 5-FU treated groups. [18F]FLT flare after 5-FU is characterized by an increase in K_1/k_2 and k_3 and a decrease in k_4. The simplified parameter, SUV_{mean} at 110-120 min after injection, can quantitatively evaluate kinetic parameters and TK1 activity after TS inhibition by 5-FU treatment. Our results suggest that [18F]FLT flare, mediated by a mechanism involving increased TK1 activity, can be used to assess the pharmacodynamics of TS inhibition by 5-FU *in vivo*. More studies are required to provide insight on the quantitative measurement of [18F]FLT flare as a valuable biomarker in selecting patients who are likely to benefit from TS inhibition.

Disclosure

The Authors declare that they have no conflict of interest.

Acknowledgements

This study was supported by a grant from the Korea Healthcare Technology R&D Project, Ministry for Health, Welfare & Family Affairs, Republic of Korea (A062254).

Table II. *Average correlation coefficients for [^{18}F]FLT kinetic parameters after vehicle or 5-fluorouracil treatment in mice implanted with HT29 tumors.*

Treatment	Parameter	V_b	K_1	K_1/k_2	k_3	k_4
Vehicle	V_b	1.00				
	K_1	–0.43	1.00			
	K_1/k_2	0.09	–0.31	1.00		
	k_3	–0.06	0.26	–0.96	1.00	
	k_4	–0.06	0.22	–0.84	0.96	1.00
5-FU	V_b	1.00				
	K_1	–0.44	1.00			
	K_1/k_2	0.25	–0.67	1.00		
	k_3	–0.15	0.53	–0.97	1.00	
	k_4	–0.02	0.18	–0.63	0.78	1.00

References

1 Meyerhardt JA and Mayer RJ: Systemic Therapy for Colorectal Cancer. New Engl J Med *352*: 476-487, 2005.

2 Smit EF, Burgers SA, Biesma B, Smit HJM, Eppinga P, Dingemans A-MC, Joerger M, Schellens JH, Vincent A, van Zandwijk N and Groen HJM: Randomized Phase II and Pharmacogenetic Study of Pemetrexed Compared With Pemetrexed Plus Carboplatin in Pretreated Patients With Advanced Non-Small-Cell Lung Cancer. J Clin Oncol *27*: 2038-2045, 2009.

3 Sargent DJ, Kohne CH, Sanoff HK, Bot BM, Seymour MT, de Gramont A, Porschen R, Saltz LB, Rougier P, Tournigand C, Douillard JY, Stephens RJ, Grothey A and Goldberg RM: Pooled safety and efficacy analysis examining the effect of performance status on outcomes in nine first-line treatment trials using individual data from patients with metastatic colorectal cancer. J Clin Oncol *27*: 1948-1955, 2009.

4 Van Cutsem E, Tabernero J, Lakomy R, Prenen H, Prausova J, Macarulla T, Ruff P, van Hazel GA, Moiseyenko V, Ferry D, McKendrick J, Polikoff J, Tellier A, Castan R and Allegra C: Addition of aflibercept to fluorouracil, leucovorin, and irinotecan improves survival in a phase III randomized trial in patients with metastatic colorectal cancer previously treated with an oxaliplatin-based regimen. J Clin Oncol *30*: 3499-3506, 2012.

5 Ford HE, Mitchell F, Cunningham D, Farrugia DC, Hill ME, Rees C, Calvert AH, Judson IR and Jackman AL: Patterns of elevation of plasma 2'-deoxyuridine, a surrogate marker of thymidylate synthase (TS) inhibition, after administration of two different schedules of 5-fluorouracil and the specific TS inhibitors raltitrexed (Tomudex) and ZD9331. Clin Cancer Res *8*: 103-109, 2002.

6 Peters GJ, van der Wilt CL, van Groeningen CJ, Smid K, Meijer S and Pinedo HM: Thymidylate synthase inhibition after administration of fluorouracil with or without leucovorin in colon cancer patients: implications for treatment with fluorouracil. J Clin Oncol *12*: 2035-2042, 1994.

7 Bianchi V, Pontis E and Reichard P: Interrelations between substrate cycles and *de novo* synthesis of pyrimidine deoxyribonucleoside triphosphates in 3T6 cells. Proceedings of the National Academy of Sciences of the United States of America *83*: 986-990, 1986.

8 Pressacco J, Mitrovski B, Erlichman C and Hedley DW: Effects of thymidylate synthase inhibition on thymidine kinase activity and nucleoside transporter expression. Cancer Res *55*: 1505-1508, 1995.

9 Gazziola C, Ferraro P, Moras M, Reichard P and Bianchi V: Cytosolic high K(m) 5'-nucleotidase and 5'(3')-deoxyribonucleotidase in substrate cycles involved in nucleotide metabolism. J Biol Chem *276*: 6185-6190, 2001.

10 Pillai RG, Forster M, Perumal M, Mitchell F, Leyton J, Aibgirhio FI, Golovko O, Jackman AL and Aboagye EO: Imaging pharmacodynamics of the alpha-folate receptor-targeted thymidylate synthase inhibitor BGC 945. Cancer Res *68*: 3827-3834, 2008.

11 Kenny LM, Contractor KB, Stebbing J, Al-Nahhas A, Palmieri C, Shousha S, Coombes RC and Aboagye EO: Altered tissue 3'-deoxy-3'-[^{18}F]fluorothymidine pharmacokinetics in human breast cancer following capecitabine treatment detected by positron emission tomography. Clin Cancer Res *15*: 6649-6657, 2009.

12 Plotnik DA, McLaughlin LJ, Krohn KA and Schwartz JL: The effects of 5-fluoruracil treatment on 3'-fluoro-3'-deoxythymidine (FLT) transport and metabolism in proliferating and non-proliferating cultures of human tumor cells. Nuclear medicine and biology *39*: 970-976, 2012.

13 Perumal M, Pillai RG, Barthel H, Leyton J, Latigo JR, Forster M, Mitchell F, Jackman AL and Aboagye EO: Redistribution of nucleoside transporters to the cell membrane provides a novel approach for imaging thymidylate synthase inhibition by positron emission tomography. Cancer Res *66*: 8558-8564, 2006.

14 Lee SJ, Kim SY, Chung JH, Oh SJ, Ryu JS, Hong YS, Kim TW and Moon DH: Induction of thymidine kinase 1 after 5-fluorouracil as a mechanism for 3'-deoxy-3'-[^{18}F] fluorothymidine flare. Biochem Pharmacol *80*: 1528-1536, 2010.

15 Wells P, Aboagye E, Gunn RN, Osman S, Boddy AV, Taylor GA, Rafi I, Hughes AN, Calvert AH, Price PM and Newell DR: 2-[^{11}C]thymidine positron emission tomography as an indicator of thymidylate synthase inhibition in patients treated with AG337. J Natl Cancer Inst *95*: 675-682, 2003.

16 Hong YS, Kim HO, Kim KP, Lee JL, Kim HJ, Lee SJ, Lee SJ, Oh SJ, Kim JS, Ryu JS, Moon DH and Kim TW: 3'-Deoxy-3'-^{18}F-Fluorothymidine PET for the Early Prediction of Response to Leucovorin, 5-Fluorouracil, and Oxaliplatin Therapy in Patients with Metastatic Colorectal Cancer. J Nucl Med *54*: 1209-1216, 2013.

17 Weber G: Biochemical strategy of cancer cells and the design of chemotherapy: G. H. A. Clowes Memorial Lecture. Cancer Res *43*: 3466-3492, 1983.
18 Cole PD, Smith AK and Kamen BA: Osteosarcoma cells, resistant to methotrexate due to nucleoside and nucleobase salvage, are sensitive to nucleoside analogs. Cancer chemotherapy and pharmacology *50*: 111-116, 2002.
19 Lehman NL and Danenberg PV: Modulation of RTX cytotoxicity by thymidine and dipyridamole *in vitro*: implications for chemotherapy. Cancer chemotherapy and pharmacology *45*: 142-148, 2000.
20 Jackman AL, Kimbell R, Aherne GW, Brunton L, Jansen G, Stephens TC, Smith MN, Wardleworth JM and Boyle FT: Cellular pharmacology and *in vivo* activity of a new anticancer agent, ZD9331: a water-soluble, nonpolyglutamatable, quinazoline-based inhibitor of thymidylate synthase. Clin Cancer Res *3*: 911-921, 1997.
21 Barthel H, Cleij MC, Collingridge DR, Hutchinson OC, Osman S, He Q, Luthra SK, Brady F, Price PM and Aboagye EO: 3'-deoxy-3'-[^{18}F]fluorothymidine as a new marker for monitoring tumor response to antiproliferative therapy *in vivo* with positron emission tomography. Cancer Res *63*: 3791-3798, 2003.
22 Lee SJ, Oh SJ, Chi DY, Kil HS, Kim EN, Ryu JS and Moon DH: Simple and highly efficient synthesis of 3'-deoxy-3'-[^{18}F]fluorothymidine using nucleophilic fluorination catalyzed by protic solvent. Eur J Nucl Med Mol Imaging *34*: 1406-1409, 2007.
23 Zimmerman RJ, VanWinkle TJ, Mantel N, Frei E 3rd and Goldin A: 5-Fluorouracil treatment of a human colon adenocarcinoma implanted in the subrenal capsule site of athymic mice. Cancer Res *46*: 694-700, 1986.
24 Makino M, Shoji H, Takemoto D, Honboh T, Nakamura S, Kurayoshi K and Kaibara N: Comparative study between daily and 5-days-a-week administration of oral 5-fluorouracil chemotherapy in mice: determining the superior regimen. Cancer Chemother Pharmacol *48*: 370-374, 2001.
25 Kim JS, Lee JS, Im KC, Kim SJ, Kim SY, Lee DS and Moon DH: Performance measurement of the microPET focus 120 scanner. J Nucl Med *48*: 1527-1535, 2007.
26 Mahteme H, Larsson BS, Sundin A and Graf W: 5-FU uptake in liver metastases after intravenous and intraperitoneal administration: an autoradiographic study in the rat. Anticancer Res *18*: 943-949, 1998.
27 Kim SJ, Lee JS, Im KC, Kim SY, Park SA, Lee SJ, Oh SJ, Lee DS and Moon DH: Kinetic modeling of 3'-deoxy-3'-^{18}F-fluorothymidine for quantitative cell proliferation imaging in subcutaneous tumor models in mice. J Nucl Med *49*: 2057-2066, 2008.
28 Choi SJ, Kim SY, Kim SJ, Lee JS, Lee SJ, Park SA, Yun SC, Im KC, Oh SJ, Kim SW, Kim JS, Ryu JS and Moon DH: Reproducibility of the kinetic analysis of 3'-deoxy-3'-[^{18}F]fluorothymidine positron emission tomography in mouse tumor models. Nucl Med Biol *36*: 711-719, 2009.
29 Muzi M, Mankoff DA, Grierson JR, Wells JM, Vesselle H and Krohn KA: Kinetic modeling of 3'-deoxy-3'-fluorothymidine in somatic tumors: mathematical studies. J Nucl Med *46*: 371-380, 2005.
30 Wells JM, Mankoff DA, Muzi M, O'Sullivan F, Eary JF, Spence AM and Krohn KA: Kinetic analysis of 2-[11C]thymidine PET imaging studies of malignant brain tumors: compartmental model investigation and mathematical analysis. Mol Imaging *1*: 151-159, 2002.
31 Hunsucker SA, Mitchell BS and Spychala J: The 5'-nucleotidases as regulators of nucleotide and drug metabolism. Pharmacol Ther *107*: 1-30, 2005.
32 Mankoff DA, Shields AF, and Krohn KA: PET imaging of cellular proliferation. Radiol Clin North Am *43*: 153-167, 2005.
33 Yau K, Price P, Pillai RG and Aboagye E: Elevation of radiolabelled thymidine uptake in RIF-1 fibrosarcoma and HT29 colon adenocarcinoma cells after treatment with thymidylate synthase inhibitors. Eur J Nucl Med Mol Imaging *33*: 981-987, 2006.

Received December 23, 2013
Revised January 17, 2014
Accepted January 20, 2014